



GREEN SYNTHESIS OF SILVER NANOPARTICLES: SPECTRAL, OPTICAL, AND ANTIBACTERIAL CHARACTERIZATION STUDIES

Helen Merina Albert*¹, S. Johnson Retnaraj Samuel², D.S. Jayalakshmi¹, C. Alosious Gonsago³

¹Department of Physics, Sathyabama Institute of Science and Technology, Chennai, Tamil Nadu, India

²Centre for Nanoscience & Nanotechnology, Sathyabama Institute of Science and Technology, Chennai, Tamil Nadu, India

³Department of Electronics Science, Mohamed Sathak College of Arts & Science, Chennai, Tamil Nadu, India

*Corresponding author: drhelenphy@gmail.com

Received: 23-03-2023; Accepted: 30-04-2023; Published: 31-05-2023

© Creative Commons Attribution-NonCommercial-NoDerivatives 4.0 International License <https://doi.org/10.55218/JASR.202314506>

ABSTRACT

A green approach was used for synthesizing Silver-NPs by the extract of *Artocarpus heterophyllus* leaves. The effect of *Artocarpus heterophyllus* leaf extract was investigated. A Powder XRD study has been used to analyze the structure and particle size of as-synthesized Silver-NPs. According to the powder-XRD study, the as-prepared Silver-NPs possess an FCC structure and have a particle size of 23nm. The possible bio-reducing agents within the leaf extracts were confirmed using FTIR spectral analysis. The characteristic surface plasmon resonance signal of the as-synthesized silver nanoparticles was detected at 450 nm using UV-Vis spectroscopic analysis between the wavelength range of 300 and 800nm. An emission peak was observed at 472nm in the PL investigation, indicating the fluorescent emission of Silver-NPs. The FESEM analysis has been exploited to inspect the morphological aspect of biosynthesized silver-NPs. According to FESEM micrographs, the biosynthesized NPs were found to have spherical shapes. Using the agar-well process, the antibacterial efficacy of biosynthesized Silver-NPs was examined. The prepared Silver-NPs exhibited a better antibacterial efficacy against *E.coli* than against *S.typhi*. It's also been observed that when the concentration increased, the antibacterial activity increased as well.

Keywords: Biosynthesis, XRD, FTIR, UV-Visible, FESEM, Antibacterial study.

1. INTRODUCTION

Nanotechnology is indeed an interdisciplinary field of study that combines key concepts from numerous fields such as physical sciences, biological sciences and engineering to develop unique methodologies for manipulating tiny particles and producing nanostructures. Nanotechnology is concerned with the production, advancement, and exploitation of a wide range of nanoparticles. Because of its applications in biology, health, biomedical, electronics, environmental sectors, sports, and the food industry, biosynthesis and characterization of metal nanoparticles is an emerging topic of nanotechnology [1-3]. Owing to the huge surface-to-volume ratio, nanoparticles have better optical properties because they can be smaller enough to trap electrons and induce quantum effects, allowing for clean detection [4]. Silver nanoparticles have remarkable physical, chemical, and organic traits amongst different metal nanoparticles. Extensive studies are being carried

out on Silver-NPs owing to their potential applications in clinical devices, pharmaceuticals, biomedical, water purification, optical, and household items [5-7]. Silver-NPs have different natural applications significantly antimicrobial, antimalarial, anti-inflammatory, wound recuperating, chemopreventive agent, and so on [8, 9]. Silver-NPs and silver-based materials are exceptionally harmful to microorganisms. Silver is known for inhibiting a wide range of bacterial strains and pathogens commonly seen in clinical and mechanical settings [10]. Since Silver-NPs have antibacterial and antifungal characteristics, they have a wide range of uses in medication development, burn infection prevention, and disinfection [11]. For the amalgamation of Silver-NPs, a variety of approaches are available, including chemical, physical, and bioreduction procedures [12, 13]. Physical and chemical techniques are rather hazardous and expensive, while biological techniques are eco-friendly, secure, and less difficult for nanoparticle synthesis [14]. The concern

with chemically producing silver nanoparticles is that they have a short lifespan owing to clustering. The silver nanoparticles generated in the majority of cases are highly unstable, necessitating the inclusion of an additional capping agent to ensure stability. Hence, due to the abrasiveness of traditional chemical procedures, biological organisms have been used to convert silver ions in solution into colloidal nanostructures. Also, with biosynthesis technique, the size characterization and toxicity of a compound can also be adjusted. It could be accomplished by employing appropriate solvents and herbal resources, such as organic products. Presently, diverse biological entities such as bacteria, fungi, yeast, plant products are extensively used in eco-friendly approaches for the generation of nanoparticles. Among the green synthesis methods, exploitation of plant extracts is an easy and clean method to synthesize metal NPs at a large scale compared with the microorganism or fungi-mediated methods. Furthermore, the leaf extracts themselves serve as capping as well as reducing agents, lowering the overall cost of the process. Plant-mediated nanoparticle synthesis is fairly quick because, unlike microbial synthesis, it does not require the use of particular media or growth conditions. Silver-NPs synthesized through this approach are quite stable because of plant peptides and proteins. The biological aspect of the biosynthesized NPs relies on different elemental features like size, shape, morphology, cell agglomeration, and reducing agent utilized in the amalgamation of nanoparticles.

Various research groups have reported green methods for synthesizing Silver-NPs by means of plant extract. According to prior reports, Silver-NPs were synthesized via leaves extract such as *Calliandra Haematocephala*, *Carica papaya*, *Carissa Carandas*, *Carya illinoensis*, *Clerodendrum inerme*, *Ixora coccinea*, *Morinda Citrifolia*, *Origanum Vulgare*, *Petalium murex*, *Petroselinum crispum*, *Prosopis Juliflora*, and *Phlomis* [15-26]. In the context of the previous works, we have used an extract of fresh *Artocarpus heterophyllus* (Jack fruit) leaves as both a bioreductant and a capping agent to synthesize silver-NPs. The jackfruit tree is a member of the mulberry family. The tropical and subtropical parts of the world, particularly Southeast Asia, are home to this tree. The fresh leaf *Artocarpus heterophyllus* offers a wide range of medicinal qualities, including diabetes prevention, antioxidant protection, and anti-aging. It's also high in potassium, which helps to keep the blood pressure and heart rate in check. Several authors have

documented the green synthesis, spectral characterization, surface morphology, and antimicrobial properties of the Silver-NPs in their backyards [27,28]. In this study, we used powder-XRD analysis to identify the structure and size of synthesized Silver-NPs, UV spectral study to confirm the formation of the compound, PL spectral study to identify the optical emission, FTIR analysis to evaluate the existence of functional groups, FE-SEM analysis to analyze the surface morphology, and antibacterial study to analyze the antibacterial effects.

2. EXPERIMENTAL

Fresh leaves of *Artocarpus heterophyllus* (Jack fruit) were harvested from the central region of kalpakkam, Tamil Nadu, India. The leaves of *Artocarpus heterophyllus* are shown in Figure 1. The recovered leaves were soaked in distilled water and dried completely to remove any dirt and other contaminating organic content. 100g of fresh leaves were finely chopped and ground, then mixed with 20ml distilled water to form a fine paste. The essence was extracted by squeezing the paste and then heated to 60 degree for an hour. The hot extract was finely filtered using 0.45 μ m filtrate once it had cooled sufficiently. The final extract has been taken in a borosil beaker and kept at room temperature.



Fig. 1: Fresh leaves of *Artocarpus heterophyllus*

The title compound was synthesized using 0.1 molar solution of AgNO_3 diluted in 40ml of distilled water. To 40ml of 0.1 molar solution of AgNO_3 , 10ml *Artocarpus heterophyllus* leaves extract was added. The mix was then thoroughly stirred for about 7-10 min at room temperature. The mixed solution changed its colour from light to brownish-black, revealing the growth of

Silver-NPs. The leaf extract of *Artocarpus heterophyllus* and observed colour change by the addition of AgNO_3 are shown in Fig.2. The synthesized nanoparticles were agitated for about 10 minutes at 10,000 rpm. Silver-NPs were collected after draining the supernatant. The obtained nanoparticles were allowed to dry after being cleaned with a little amount of ethanol and heated in Mantle Heaters. The prepared NPs were used for further characterization studies.

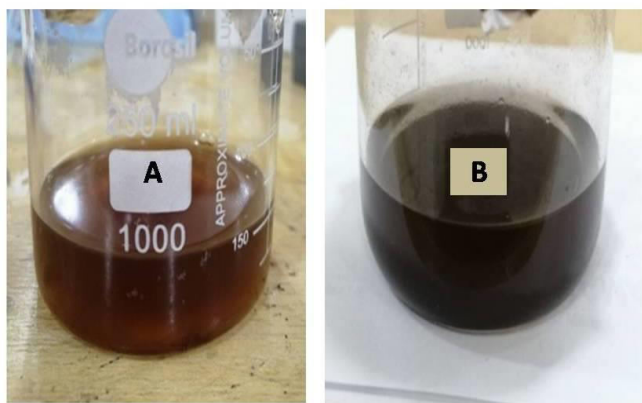


Fig. 2: (a) Leaf extract of *Artocarpus heterophyllus* (b) AgNO_3 -induced color shift

3. RESULTS AND DISCUSSION

3.1. Powder-XRD Method

Powder-XRD analytical method has been employed to confirm the formation and the structure of green synthesized Silver-NPs. Figure 3 illustrates the plot of XRD data of green synthesized Ag-NPs. In this plot, prominent peaks were indexed based on the FCC structural report (JCPDS file no 04-0783). Silver-NPs have intense diffraction peaks at (111), (200), (220), and (113), which correspond to the two theta values of 38.09, 46.37, 64.66, and 77.2 degrees, correspondingly. Data acquired for the peaks is consistent with the FCC structural report (JCPDS file no 04-0783). The Debye-Scherrer equation $D = k\lambda/\beta\cos\theta$ has been applied to compute the typical size of the NPs [29]. In the equation, D denotes the particle size determined from the XRD plot, θ denotes Bragg's angle in degrees, λ denotes X-ray's wavelength, β denotes angular width of the diffraction pattern about half maximum, and k denotes the constant of Debye-Scherrer equation. In this analysis, the typical size of the synthesized samples has been determined to have around 23nm. Moreover, the appearance of diffraction patterns, as well as the average particle size (23nm), clearly shows that Ag-NPs are formed by this green procedure.

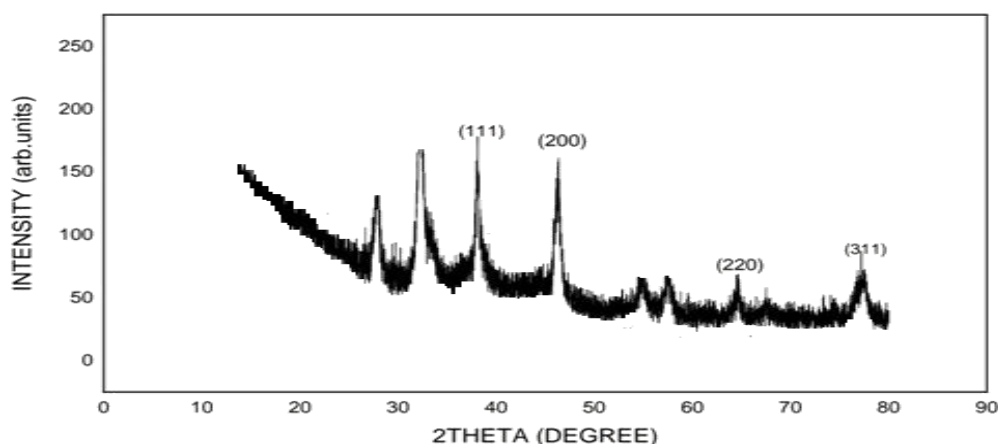


Fig. 3: Powder XRD spectrum of green synthesized Silver-NPs

3.2. FT-IR Spectroscopy

FT-IR is the constructive spectroscopic technique of providing information about the chemical bonding of solids and thin films [30]. The presence of bio-molecules and stability of the metal NPs were identified using FT-IR measurements. Figure 4 illustrates the FT-IR spectra of the synthesized nanoparticles. Absorbance bands of *Artocarpus heterophyllus* are found near 3304cm^{-1} for O-H

stretch, 2164cm^{-1} for C=C alkynes stretch, 1980cm^{-1} for C-H aromatic bending, 1633cm^{-1} for C=O amides stretch, 1381cm^{-1} for C-H alkane bend, and 963cm^{-1} for C=C alkene bend. According to the FTIR analysis, the carboxylic acid (-OH), Aromatic (C-H), and Amides (C=O) groups of *Artocarpus heterophyllus* leaves extract are primarily engaged in the transformation of Ag^+ to Silver-NPs.

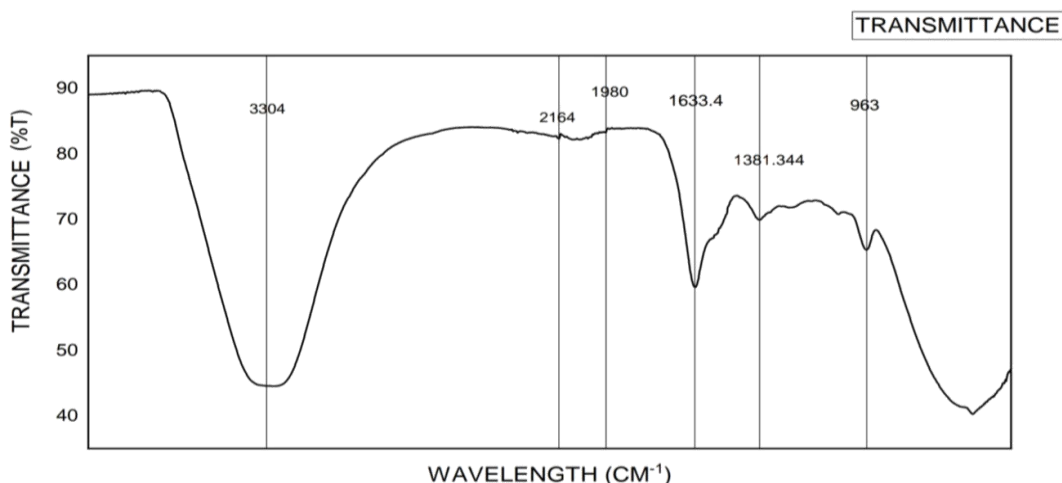


Fig. 4: FT-IR spectrum of Silver-NPs

3.3. UV-Vis Spectral Study

UV-Vis spectral analysis is used for measuring the magnitude of a wavelength absorbed by a given material in the UV-Visible range [31]. A Jasco UV-Vis-NIR spectrophotometer with a scan rate of $200\text{nm}\cdot\text{min}^{-1}$ was used for UV-Vis analysis. UV-Visible spectrum recorded in an aqueous solution between the wavelength ranges 300 to 800nm was used to evaluate the development of the reaction involving metal ions as well as the leaves extract.

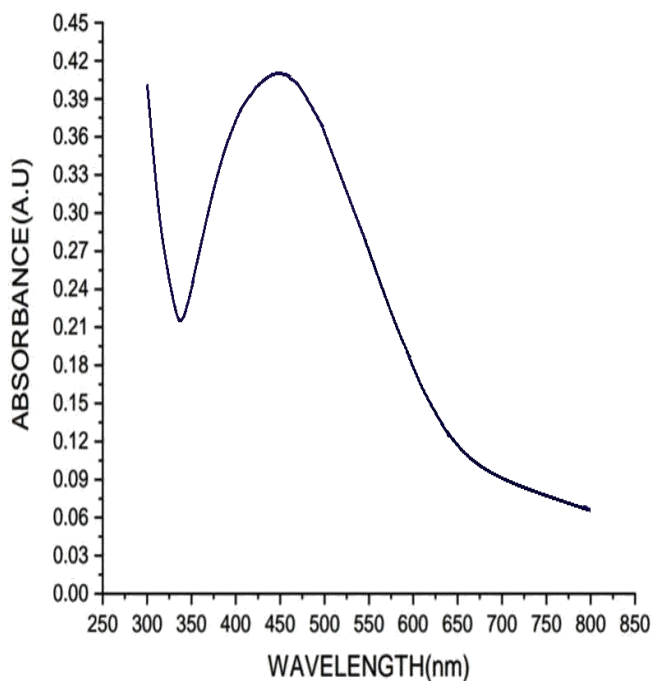


Fig. 5: UV-Vis curve of Silver-NPs

Figure 5 illustrates UV-Visible waveform of silver-NPs. An intensive characteristics absorbance peak near 450nm has been found in this curve. This characteristic absorbance peak is because of Surface Plasmon Resonance (SPR) effect within synthesized sample [32-34]. An important feature of silver-NPs is that the resonance peak may appear in the wavelength range 400 to 570nm. As a result, the generation of silver -NPs is well documented by the occurrence of the SPR peak near 450nm in the recorded spectra. Previously, it has been reported that the appearance of resonance peaks in the range 400-450nm of UV-Vis spectrum correspond to the metal NPs with a spherical form [35]. In our case, occurrence of a resonance peak around 450nm there in UV curve confirms that silver-NPs are spherical, which agrees well with our FESEM investigation.

3.4. Photoluminescence Study

Photoluminescence spectroscopy (PL) is a versatile method for analysing a compound's electronic structure and optical properties [36]. The colloidal Silver-NPs were uniformly dispersed in an aqueous solution, and the corresponding spectrum was obtained for the excitation wavelength of 420nm. The recorded PL spectrum of green synthesized Silver-NPs from *Artocarpus heterophyllus* leaves extract is illustrated in Figure 6. From the plot, a highly intensive emission peak has been observed at 472nm. After that, the intensity of emission gradually decreases upto 600nm and reaches a minimum. Jiang et al. have reported that the emission peak in the water phase was formed at 465nm in the PL spectra [37]. Hence, in the present

case, the emission peak formed at 472nm in the PL spectrum is slightly red-shifted.

3.5. FE-SEM Analysis

FE-SEM technique is used to detect structures as small as 1nm and to visualize the topographic details of any objects. For this purpose, prepared samples were coated with an extremely thin layer (2nm) of gold palladium. The coating on the sample forms a conductive layer which improves the secondary electron signals and also protects the sample from overheating. The morphology of the sample is replicated by the appearance of a real-time image on the FE-SEM screen. Fig. 7 illustrates the FE-SEM micrographs of the green synthesized Ag-NPs. Fig. 7a illustrates the observation of the nanoparticles at 30.0 K X magnification; Fig. 7b illustrates the view at 50.0 K X magnification; Fig. 7c at 80.0 K X magnification and

the Fig. 7d at 100.0 K X magnification over the width of 5.8mm of the sample at the working voltage of 5KV. The FE-SEM micrographs (Fig. 7a & b) confirm the agglomeration of nanostructural homogeneities over the surface, with a particle size of 23nm on average.

Micrographs (Fig. 7c & d) show that the detected NPs are nearly spherical shape, which is consistent with previous investigations [38].

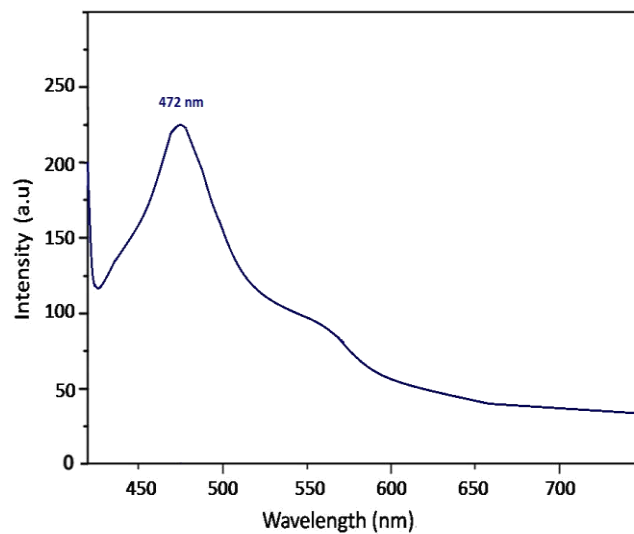


Fig. 6: PL spectrum of Silver-NPs

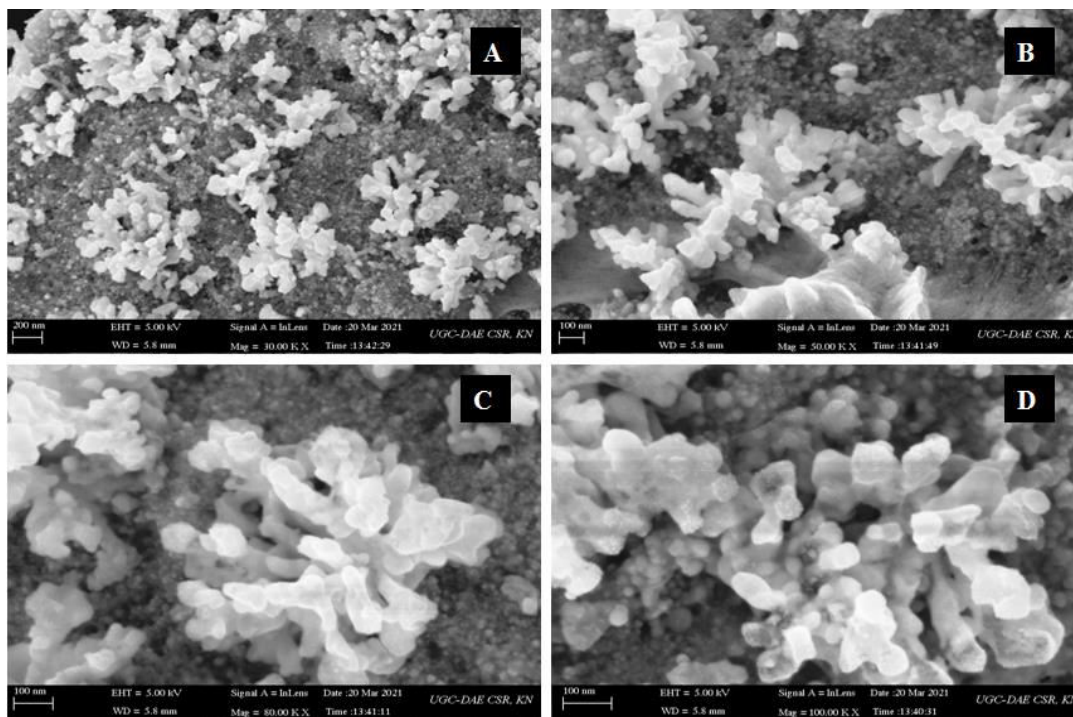


Fig. 7: FE-SEM micrographs of Silver-NPs with different magnifications

3.6. Antibacterial Study

Silver-NPs have emerged as an effective antibacterial against multidrug-resistant bacteria because of its huge surface-to-volume ratio in addition to the distinctive physiochemical characteristics [39]. Moreover, Silver-

NPs can pass through bacterial cell walls, altering the structure of cellular membranes and even perhaps resulting in cell death [40]. The antibacterial ability of biosynthesized Silver-NPs against two bacterial species, *Escherichia coli* and *Salmonella typhi*, was examined in

this study using Mueller-Hinton agar plates. Briefly, sterile agar medium was poured in a sterile petridish aseptically and allowed for solidification for 30 minutes. Over-night bacterial culture was inoculated in the medium, and Silver-NPs were loaded in the well and the dishes were incubated with 37°C about 24 h in bacterial incubator. Just following the incubation time, the zone of inhibition was identified surrounding the well. Antibacterial ability of the biosynthesized Silver-NPs had been observed by determining the diameter of the zone of inhibition. Antibacterial ability of the biosynthesized Silver-NPs had been tested for three

distinct concentrations 20, 40 and 60µl. Briefly, *E. coli* has shown the zone of inhibition for 20µl, 40µl and 60µl loaded Silver-NPs samples as 6mm, 10mm and 12mm, respectively. Similarly, we have performed the antibacterial effect of synthesized NPs against *S.typhi*, and the inhibition zone was noted for 20µl, 40µl and 60µl loaded Ag-NPs samples as 4mm, 7mm and 9mm, correspondingly, and are shown in Fig. 8. According to the findings, the biosynthesized Silver-NPs had more effective antibacterial action against *E.coli* than against *S.typhi*. Also, it has been observed that the antibacterial activity increases by increasing the concentration.

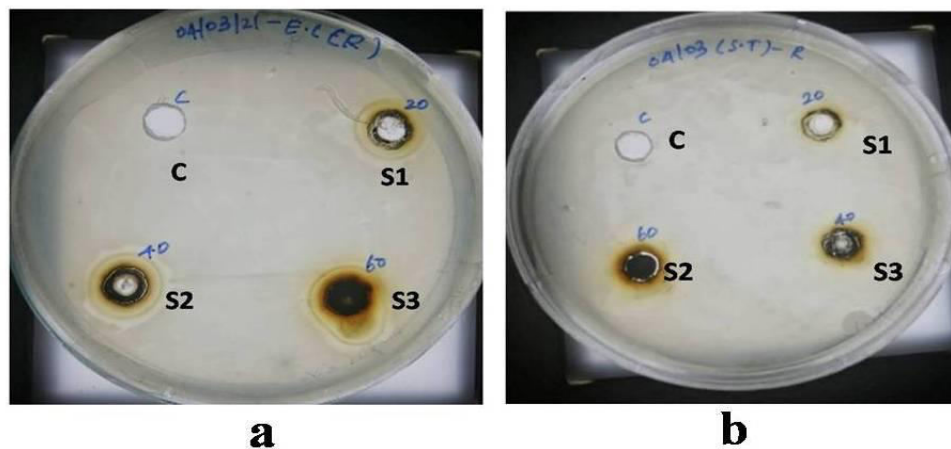


Fig. 8: Antibacterial ability against (a) E. Coli, and (b) S. typhi for 20µl, 40µl, and 60µl Ag-NPs

4. CONCLUSION

In this investigation, we adopted a green technique to synthesise Silver-NPs, by means of *Artocarpus heterophyllus* leaves extract. Powder XRD analysis, FT-IR spectroscopy, UV-Visible spectroscopy, PL study, FE-SEM analysis, and antibacterial assays have been used to further characterise the nanoparticles. According to powder XRD analysis, the green synthesized Ag-NPs possess FCC structure and have particle size 23nm. FTIR spectroscopic analysis confirmed the existence of functional groups and generation of Ag-NPs. In UV-Vis absorption curve, the SPR Peak was observed around 418nm, revealing the amalgamation of Ag-NPs. In PL spectral investigation, the green synthesized nanoparticles were found to be photo-luminescent with an emission peak at 472nm that was slightly red-shifted. FE-SEM analysis revealed that the surface of the biosynthesized nanoparticles seemed to be spherical in shape. *Artocarpus heterophyllus* leaves extract-assisted green synthesized Silver-NPs have shown significant antibacterial efficacy against gram-negative pathogens in

an antibacterial assay. Based on our investigation, *Artocarpus heterophyllus* leaves extract-assisted green synthesized Silver-NPs might be used as a coating in surgical tools and hand tools to avoid especially gram-negative bacterial contamination.

Conflicts of interest

Nil

Source of Funding

The authors declare that no funds, grants, or other support were received during the preparation of this manuscript.

5. REFERENCES

1. Mughal, B, Zaidi SZJ, Hassan SU. *Appl Sci*, 2021; **11**:2598.
2. Mariappan N. *Biomed Pharmacol*, 2019; **12**:1095-1127.
3. Gawande MB, Goswami A, Felpin FX, Asefa T, Huang X, Silva R, et al. *Chem Rev*, 2016; **116**:3722-3811.

4. Sharma PC, Sharma D, Sharma A, Saini N, Goyal R, Ola M, et al. *Mat Today Chem*, 2020; **18**:100349.
5. Burdusel AC, Gherasim O, Grumezescu AM, Mogoanata L, Ficai A, Andronesu E, et al. *Nanomater*, 2018; **8**:681.
6. Valentina M, Luisana DC, Stephen GJS, Simona O, Magda B, Anna LC, et al. *Soc Open Sci*, 2018; **5**:171113.
7. Zhang XF, Lui ZG, Shen W, Gurunathan S. *Int J Mol Sci*, 2016; **17**:1534.
8. Shavandi A, Saeedi P, Azam Ali M, Jalalvand E. *Funct Poly Biomed Appl*, 2019; 1263-1271.
9. Tavaf Z, Tabatabaei M, Khalafi-Nezhad A, Panahi F. *Eur J Intergr Med*, 2017; **12**:163-171.
10. Wang L, Hu C, Shao L. *Int J Nanomed*, 2017; **12**:1227-1249.
11. Deshmukh SP, Patil SM, Mullani SB, Delekar SD. *Mater Sci Eng C Mater Biol Appl*, 2019; **97**:954-965.
12. Henriquez LC, Alfaro KA, Alvarez JU, Fernandez LV, de Oca Vasquez GM, Baudrit JRV. *Nanomater*, 2020; **10**:1763.
13. Shah M, Fawcett D, Sharma S, Tripathy SK, Poinern GEJ. *Materials (Basel)*, 2015; **8**:7278-7308.
14. Sastry M, Ahmed A, Khan MI, Kumar R. *Curr Sci*, 2003; **85**:162-170.
15. Raja S, Ramesh V, Thivaharan V. *Arab J Chem*, 2017; **10**:253-261.
16. Syafiuddin A, Salmiati, Hadibarata, Salim MR, Kueh ABH, Sari AA. *Bioprocess Biosys Eng*, 2017; **40**:28597212.
17. Singh R, Hano C, Nath G, Sharma B. *Biomol*, 2021; **11**:299.
18. Dalir SJB, Djahaniani H, Nabati F, Hekmati M. *Heliyon*, 2020; **6**: e03624.
19. Khan SA, Shahid S, Lee CS. *Biomol*, 2020; **10**:835.
20. Karuppiyah M, Rajmohan R. *Mat Lett*, 2013; **97**:141-143.
21. Asha RP, Kavitha S, Sheweta S, Priyanka P, Vrinda A, Vivin TS, Silpa S. *Int J Pharm Pharma Sci*, 2015; **7**:459-461.
22. Shaik MR, Khan M, Kuniyil M, Al-Warthan A, Alkathlan HZ, Siddiqui MRH, et al. *Sustainability*, 2018; **10**:913.
23. Anandalaksmi J, Venugobal J, Ramasamy V. *Appl Nanosci*, 2016; **6**:399-408.
24. Roy K, Sarkar CK, Ghosh CK. *Appl Nanosci*, 2015; **5**:945-951.
25. Raja K, Saravanakumar A, Vijayakumar R. *Spectrochim Acta A*, 2012; **97**:490-494.
26. Allafchian AR, Mirahmadi zare SZ, Jalai SAH, Hashemi SS, Vahabi MR. *J Nanostruct Chem*, 2016; **6**:129-135.
27. Rautela A, Rani J, Debnath D. *J Anal Sci Techol*, 2019; **10**:5.
28. Ijaz I, Gilani E, Nazir A, Bukhari A. *Green Chem Lett Rev*, 2020; **13**:223-245.
29. Ganesh Kumar C, Pombala S, Poornnachandra Y, Agarwal SV, Nanomaterials in antimicrobial therapy. New York: William Andrew Publishing; 2016.
30. Alosious Gonsago C, Helen Merina Albert, Karthikeyan J, Sagayaraj P, Joseph Arul Pragasam A. *Mat Res Bull*, 2012; **47**:1648-1652.
31. Jose Chirayil C, Abraham J, Mishra RK, George SC, Thomas S. In: Thomas S, Thomas R, Zachariah A, Mishra R, editors. Thermal and Rheological Measurement techniques for Nanomaterials Characterization. Amsterdam: Elsevier Publishing; 2017.
32. Link S, Ei Syed MA, *Ann Rev Phys Chem*, 2003; **54**:331-366.
33. De Leersnyder I, Rijckaert H, De Gelder L, Van Driessche I, Vermeir P. *Nanomater*, 2020; **10**:1394.
34. Taleb A, Petit C, Pllen MP. *J Phy Chem B*, 1998; **102**:2214-2220.
35. Prathna TC, Chandrasekaran N, Raichur AM, Mukherjee A. *Coll Surf B Biointerf*, 2011; **82**:152-159.
36. Helen Merina Albert, Lohitha T, Karthik Alagarsamy, Alosious Gonsago C, Vinita V. *Mater Today Proc*, 2021; **47**:1030-1034.
37. Jiang Z, Yuan W, Pan H. *Spectrochim Acta A*, 2005; **61**:2488-2494.
38. Sathishkumar G, Gopinath C, Karpagam K, Hemamalini V, Premkumar K, Sivaramakrishnan S. *Coll Surf B Biointer*, 2012; **95**:235-240.
39. Rabbi MA, Rahman MM, Minami H, Habib MR, Ahmad H. *Carbohydrate Polym*, 2020; **233**:115842.
40. Lok CN, Ho CM, Chen R, He QY, Yu WY, Sun H, et al. *J Prote Res*, 2006; **5**:916-924.